VISUALISING MUSCLE ANATOMY USING THREE-DIMENSIONAL COMPUTER MODELS - AN EXAMPLE USING THE HEAD AND NECK MUSCLES OF *SPHENODON*

Neil Curtis, Marc E. H. Jones, Susan E. Evans, Paul O'Higgins, and Michael J. Fagan

ABSTRACT

We demonstrate how the computer-based technique of multi-body dynamics analysis (MDA) can be used to create schematic, but informative three-dimensional (3D) representations of complex muscle anatomy. As an example we provide an overview of the head and neck muscles present in *Sphenodon* (Diapsida: Lepidosauria: Rhynchocephalia). First a computer model based on micro-computed tomography datasets provides a detailed and anatomically correct three-dimensional (3D) framework to work from. Secondly, muscles are represented by groups of cylinders that can be colour coded as desired. This allows muscle positions, attachment areas, and 3D orientation to be visualised clearly. This method has advantages over imaging techniques such as two-dimensional drawings and permits the form and function of the muscles to be understood in a way that is not always possible with more classical visualisation techniques.

Neil Curtis. Department of Engineering, University of Hull, Hull, HU6 7RX, United Kingdom. n.curtis@hull.ac.uk.

Marc E. H. Jones. Research Department of Cell and Developmental Biology, Gower Street, UCL, University College London, London, WCIE 6BT, United Kingdom. marc.jones@ucl.ac.uk.

Susan E. Evans. Research Department of Cell and Developmental Biology, Gower Street, UCL, University College London, London, WCIE 6BT, United Kingdom. ucgasue@ucl.ac.uk.

Paul O'Higgins. The Hull York Medical School, University of York, York, YO10 5DD, United Kingdom. paul.ohiggins@hyms.ac.uk.

Michael J. Fagan. Department of Engineering, University of Hull, Hull, HU6 7RX, United Kingdom. m.j.fagan@hull.ac.uk.

KEY WORDS: 3D; imaging; muscle; myology; head; neck

INTRODUCTION

In the past, muscles were mainly described and illustrated using monochrome line drawings often in a standard anatomical plane such as lateral view (e.g., Byerly 1925; Oelrich 1956; Haas 1973; Schumacher 1973; Gomes 1974; Wu 2003). The limitations are obvious when describing complex three-dimensional (3D) structures and may lead to ambiguous communication or misunderstandings. For example, Gorniak et al. (1982) provide a detailed illustration of the jaw muscles in *Sphenodon* (Günther 1867), but it is ambiguous as to the path of the muscle labelled as m. Adductor Mandibulae Externus Posterior and, indeed, it is uncertain whether this muscle is correctly identified (Wu 2003; Jones et al. 2009). From drawings made in lateral view alone it is also often difficult to appreciate the mediolateral orientation of muscles, for example the complexities of the pterygoideus muscle in the lizard *Uromastyx* (e.g., Haas 1973; Throckmorton 1978).

Hypotheses for the muscle arrangement in fossil taxa have long been carried out (e.g., Adams 1919; Anderson 1935; Fox 1964; Barghusen 1973; Rieppel 2002), with the depiction and communication of such hypotheses being subject to similar problems. More recent descriptions of muscle anatomy include photographic images on to which muscle groups are drawn and colour coded (e.g., Sniverly and Russell 2007; Tsuihiji 2007), and improve the clarity and understanding of muscle positioning and function.

Computer-based data collection and imaging has been used to some extent by palaeontologists and comparative anatomists for at least 25 years (e.g., Conroy and Vannier 1984; Conroy et al. 1990), but only with the recent advances in computational power have 3D imaging and functional analysis become more widespread (e.g., Hutchinson et al. 2005; Motani 2005; Grosse et al. 2007; Wickens 2007; Strait and Evans 2008; Sutton 2008). Examples include the description of the cranial anatomy of dinosaurs, which has been impressively presented in recent publications (Witmer and Ridgely 2008, 2009; Evans et al. 2009), and 3D bony anatomy derived from computed tomography (CT) data of dinosaur skulls that has been used as a frame on which to present muscle anatomy (e.g., Holliday 2009).

The modelling and analysis software known as multi-body dynamics analysis (MDA) is an engineering technique that has recently been used to calculate the kinetic and kinematic behaviour within skulls (e.g., Curtis et al. 2008, 2009; Moazen et al. 2008, 2009). Although not the primary purpose of this software, the way in which muscles are generated has the potential to make the muscle anatomy more clear and to help understand the function of individual muscle groups. Others apply this technology to understand function (e.g., Hutchinson et al. 2005), but the potential of this technique as a pure visualisation tool has not yet been explored or highlighted.

In order to demonstrate this potential, we present a thorough treatment of the head and neck muscles in *Sphenodon*. As the only extant rhynchocephalian (*sensu* Gauthier et al. 1988) this genus is an important reference taxon for work on the muscles of other amniotes (Schwenk 1986; Bryant and Russell 1992; Witmer 1995; Abdala and Moro 2003; Holliday and Witmer 2007), and it is therefore important that anatomical interpretations are both clear and detailed. The muscle arrangements of *Sphenodon* have been repeatedly examined and discussed (e.g., Nishi 1916; Byerly 1925; Anderson 1936; Poglayen-Neuwall 1953; Haas 1973; Gorniak et al. 1982; Wu 2003), although, as for many other taxa, they have mainly been described and illustrated in lateral view using line drawings. Apart from a few recent examples (e.g., Tsuihiji 2005, 2007; Holliday and Witmer 2007; Jones et al. 2009), authors were restricted to monochromatic images (e.g., Poglayen-Neuwall 1953; Haas 1973), and as descriptions have become more detailed, the limitations of these methods have become more apparent.

Here accurate 3D models of the skull, lower jaw, and neck of *Sphenodon* form a base on to which muscle groups are positioned. The muscles are represented as simple cylinders and thus allow the origins and insertions to be easily identified. Complex muscle groups are divided into clear, colour coded sections. A variation in bone transparency and orientation are used to achieve the best view of the muscle attachment, and the effective lines of action can be determined for each muscle group in both lateral and anterior views.

This paper visually presents all muscle groups in *Sphenodon* with only limited descriptive text; the muscle arrangements are based on a comprehensive descriptive review published by Jones et al. (2009).

MATERIALS AND METHODS

A dry *Sphenodon* skull (specimen LDUCZ x036) was subjected to micro-computed tomography (micro-CT) at the University of Hull, UK. Then, using image segmentation and analysis software

(AMIRA 4.1, Mercury Computer Systems Inc., USA), the micro-CT dataset was converted into 3D models of the skull and lower jaws. An additional micro-CT dataset (University of Texas, Austin, USA) was used in the construction of the neck (specimen YPM 9194). This additional dataset required some manipulation as the neck was twisted and only part of the 6th vertebra was scanned. With reference to other dry *Sphenodon* material (LDUCZ x036) the proatlas and the first two vertebrae (atlas and axis) were subsequently realigned during the 3D model construction, and the right-hand portion of the most posterior vertebra and girdle were duplicated and mirrored to form a complete and symmetrical structure. The soft tissue fascia sheets that cover the lower temporal fenestra (onto which part of the adductor musculature attaches) were created manually in AMIRA, and the 7th and 8th vertebrae of the neck were simply represented by cylinders and cuboids positioned posterior to the 6th vertebra. These 3D models were imported into ADAMS multi-body dynamics software (MSC Software Corp, USA), in which a representation of the muscle groups were added.

Each muscle group is represented by several straight cylinders extending between the skull and lower jaw, or skull and neck. The exact origin and attachment point of each cylinder was positioned according to descriptions in Jones et al. (2009), which was, in turn, based on descriptions in the works of previous authors (e.g., Nishi 1916; Byerly 1925; Anderson 1936; Poglayen-Neuwall 1953; Haas 1973; Gorniak et al. 1982; Wu 2003; Al-Hassawi 2004, 2007; Tsuihiji 2005, 2007; Holliday and Witmer 2007) in combination with first-hand observations. When a muscle wraps around other muscles or bone, it is represented by two or three cylinders joined end-to-end. The colour coding and abbreviations used in this paper follow as closely as possible those of Jones et al. (2009).

MUSCULATURE

Jaw Muscles

Table 1 summarises all major jaw closing and opening muscle groups associated with *Sphenodon*. Brief descriptions of the main function of each individual muscle group are presented in Table 1, but for a comprehensive review of muscle function and anatomy see Jones et al. (2009). Figure 1 presents all adductor muscles covered in this paper, while Figures 2 - 12 each represent select groups of muscles, as identified in Table 1.

Neck Muscles

Portions of some neck muscles extend between neighbouring vertebrae and provide stability for the axial skeleton (e.g., Byerly 1925; Gasc 1981; Tsuihiji 2005, 2007); however, it is only the sections of the muscle that extend anteriorly and attach directly to the skull that will be considered here. Table 2 lists these neck muscles along with their main contribution towards head movements. Figure 13 presents all neck muscles in *Sphenodon*, while Figures 14 - 20 represent select groups of neck muscles, as identified in Table 2.

SUMMARY

Multi-body dynamics analysis (MDA), a 3D engineering technique, was used here as a visualisation tool to present the head and neck musculature of *Sphenodon*. Figure 21 displays the entire muscular anatomy of the *Sphenodon* head and includes all individual muscle groups covered in this paper. Alternatively, a rotating movie of the 3D *Sphenodon* model with all musculature is shown in Figure 22, while a rotating movie with superficial muscle groups removed is shown in Figure 23. The colour coding is consistent in all images and matches, as far as possible, that was used elsewhere (e.g., Tsuihiji 2005, 2007; Holliday and Witmer 2007; Jones et al. 2009). The detailed muscle anatomy is presented in a clear, simple manner, where muscle groups are divided into a finite number of sections, each represented by one to three straight cylinders. The ability to display a 3D representation (from any view) of colour coded muscle groups, and the option of removing or altering the transparency of specific objects means that the muscle origin/ insertion locations and muscle force lines of action can be visualised clearly.

In reality muscles bulge, wrap, and blend into tendons; they are therefore more complex in terms of their structure than represented here. Nevertheless, the presentation of muscles in this paper allows the general role of each individual muscle group to be determined based on its location, and the relative interaction between muscle groups to be inferred. For example, from Figure 14 we see that the m. Episternocleidomastoid (mEscm, red) follows on from the m. Clavicle Dorsalis (mClDo, peach) and the m. Trapezius (mTrap, purple) to form a strong collar of muscle that connects the girdle and neck with the posterior regions of the skull. We can then infer that these muscles together contribute to raising and turning/ twisting the head, as well as contributing to general head stability during

TABLE 1. Summary of all jaw muscles modelled in this paper.

Muscle Group	Figure	Muscle Colour	Sections	Wrapping	Muscle Function
m. Adductor Mandibulae Externus Superficialis (mAMES) sensu stricto	2	Light Blue	14	No	Closes the jaw.
m. Adductor Mandibulae Externus Medialis (mAMEM)	3	Light Purple	5	No	Closes the jaw and some posterior translation of the mandible.
m. Adductor Mandibulae Externus Profundus (mAMEP)	4	Purple	5	No	Closes the jaw and some posterior translation of the mandible.
m. Pseudotemporalis Superficialis (mPstS)	5	Pink	4	No	Closes the jaw.
m. Pseudotemporalis Profundus (mPstP)	5	Yellow	2	No	Closes the jaw.
m. Pterygoideus Typicus (mPtTyp) - Deep	6 & 7	Red	2	No	Closes the jaw and anterior translation of the mandible.
m. Pterygoideus Typicus (mPtTyp) - Medial Middle	6 & 7	Green Yellow	5	No	Closes the jaw and some anterior translation of the mandible.
m. Pterygoideus Typicus (mPtTyp) - Lateral Middle	6 & 7	Orange	3	Yes	Closes the jaw and anterior translation of the mandible.
m. Pterygoideus Typicus (mPtTyp) - Ventrolateral	6 & 7	Brown Red	1	Yes	Closes the jaw and anterior translation of the mandible.
m. Pterygoideus Atypicus (mPtAty)	8	Gold	3	Yes	Closes the jaw and anterior translation of the mandible.
m. Adductor Mandibulae Posterior (mAMP)	9	Dark Green	5	No	Closes the jaw and posterior translation of the mandible.
m. Levator Pterygoidei (mLPt)	10	Green	3	No	Connection between orbitosphenoid and epipterygoid base.
m. Protractor Pterygoidei (mPPt)	11	Magenta	4	No	Connects the braincase to the quadrate-pterygoid wing and epipterygoid (may be involved in cranial kinesis)
m. Depressor Mandibulae (mDM) Lateral	12	Dark Gray	2	Yes	Opens the jaw.
m. Depressor Mandibulae (mDM) Medial	12	Light Gray	2	Yes	Opens the jaw.

activities such as feeding or locomotion. Assessing the jaw adductor muscles, we can suggest that the vertical alignment of the m. Adductor Mandibulae Externus Superficialis (mAMES, Figure 2.1) renders it well placed to move the lower jaw orthally (Olson 1961), whereas the more angled m. Pterygoideus Typicus (mPtTyp, Figures 6 and 7) will contribute more towards anterior translations of the mandible.

The method of representing muscle anatomy presented here is not intended to replace more classical techniques such as line drawings for depicting observed or hypothesised muscle anatomy. The visual representations do however offer an additional and complimentary means of communicating such morphological information, and may appeal to scientists who do not have extensive experience in muscle anatomy and function.
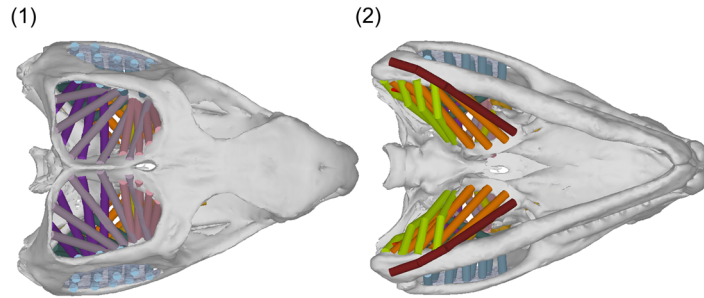
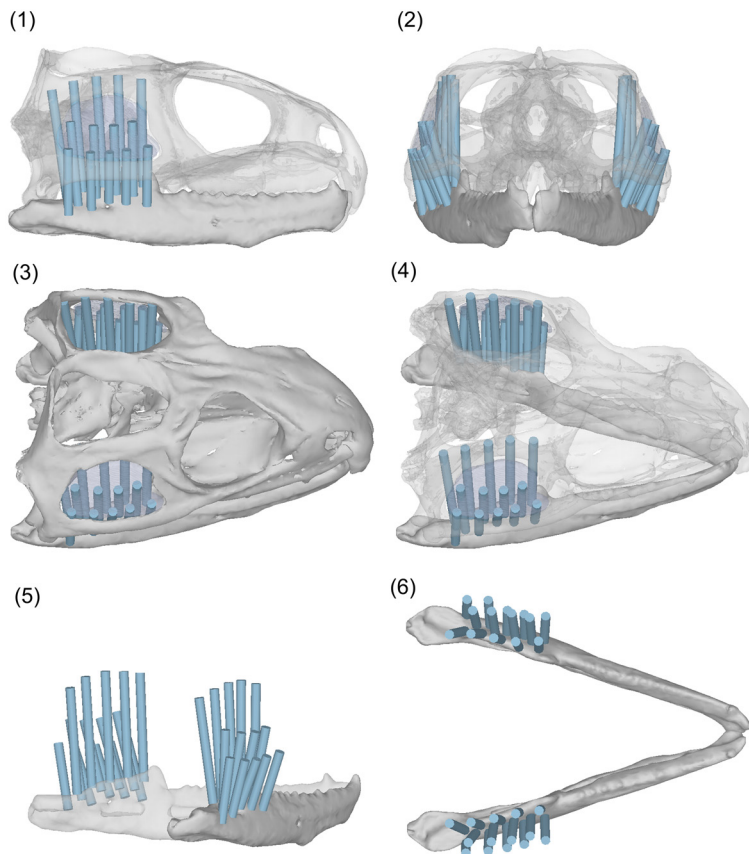**FIGURE 1.** (1) Dorsal and (2) ventral views of the adductor mandibulae muscular arrangement.

FIGURE 2. mAMES. (1) Lateral view with the skull at 80% transparency; (2) anterior view with the skull at 80% transparency; (3) dorsolateral view; (4) dorsolateral view with the skull at 80% transparency; (5) posterolateral view without the skull and the far side of the lower jaw at 60% transparency; (6) dorsal view without the skull. Where present the fascia is at 80% transparency.
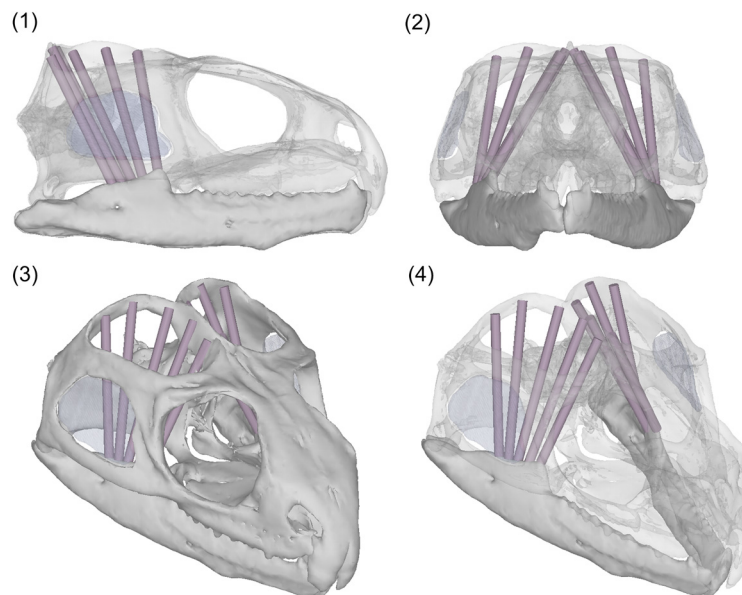
FIGURE 3. mAMEM. (1) Lateral view with the skull at 80% transparency; (2) anterior view with the skull at 80% transparency; (3) anterolateral view; (4) anterolateral view with the skull at 80% transparency. The fascia is at 80% transparency.
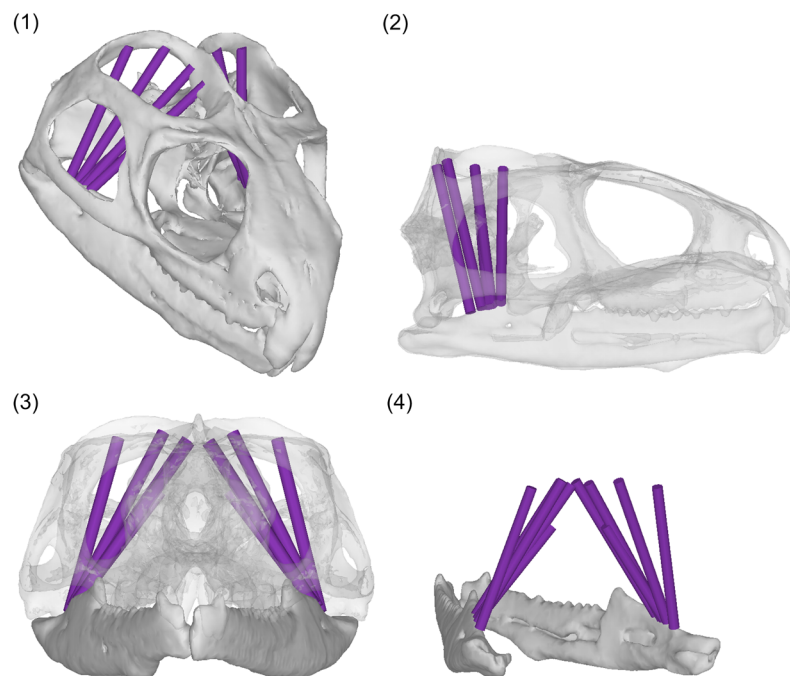
FIGURE 4. mAMEP. (1) Anterodorsolateral view; (2) lateral view with all bone at 80% transparency; (3) anterior view with the skull at 80% transparency; (4) posterolateral view showing only the lower jaw. The fascia is not visible in this figure.
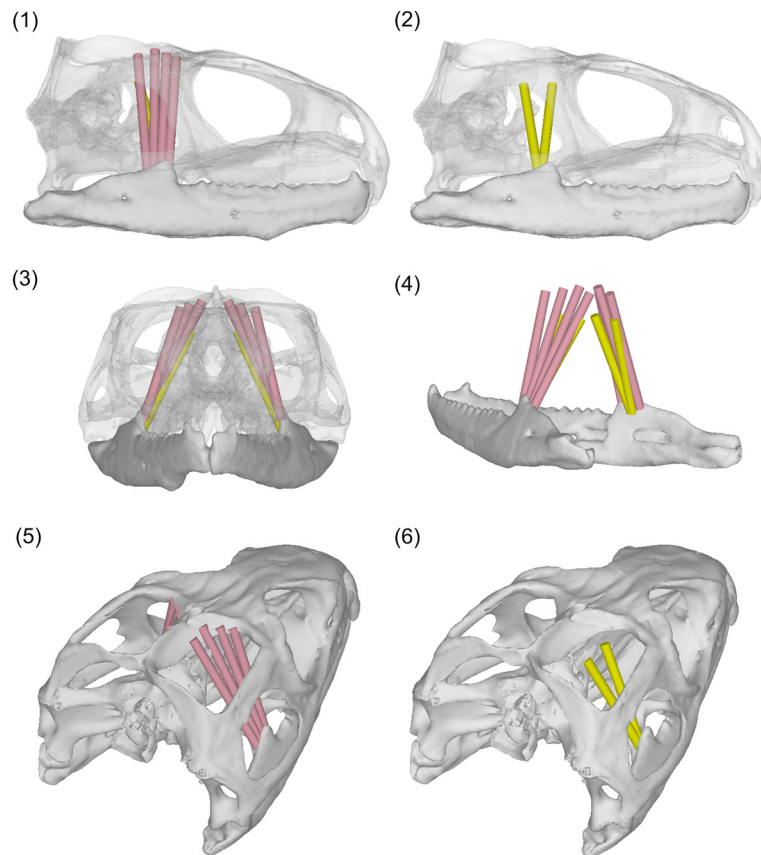
FIGURE 5. mPstS (pink) and mPstP (yellow). (1) Lateral view showing both the mPstS and mPstP with the skull at 80% transparency; (2) lateral view showing only the mPstP with the skull at 80% transparency; (3) anterior view showing both the mPstS and mPstP with the skull at 80% transparency; (4) posterolateral view of only the lower jaw showing both the mPstS and mPstP; (5) posterodorsolateral view of the mPstS; (6) posterodorsolateral view of the mPstP. The fascia is not included in this figure.
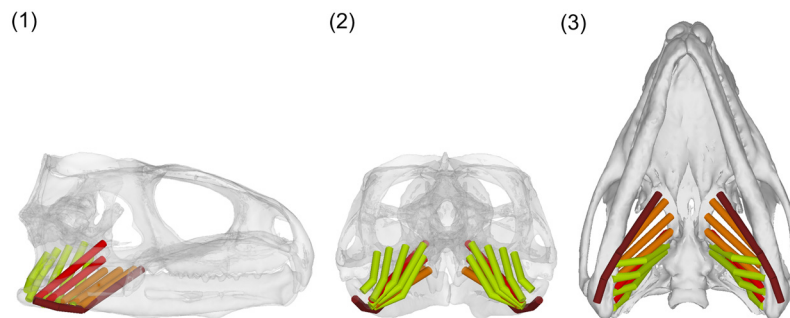

FIGURE 6. m. Pterygoideus. (1) Lateral view with all bone at 80% transparency; (2) posterior view with the skull and lower jaws at 80% transparency; (3) ventral view. Figure includes the dorsal (red), middle (orange and green yellow) and ventrolateral (brown red) portions of the mPtTyp. No fascia is present in this figure.
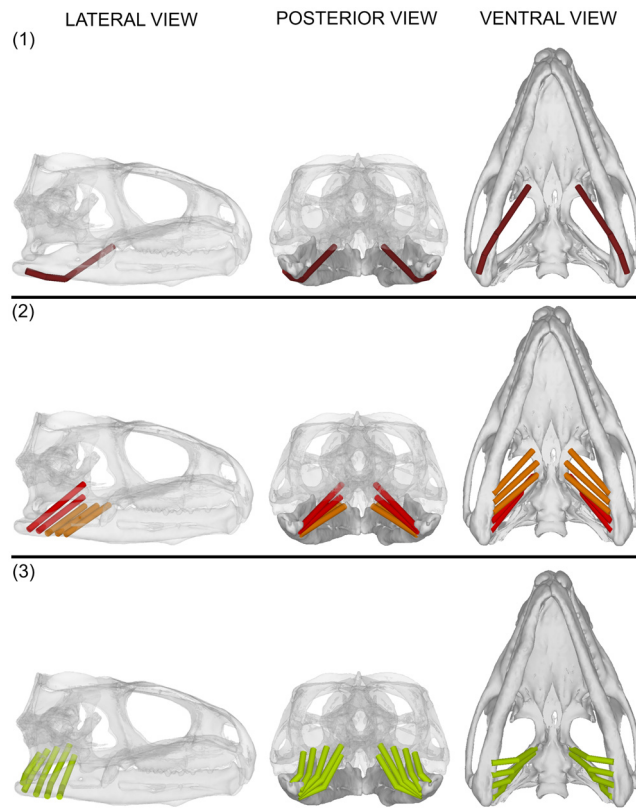
LATERAL VIEW   POSTERIOR VIEW   VENTRAL VIEW

FIGURE 7. mPtTyp. Lateral, posterior and ventral views of (1) ventrolateral (brown red) portion of the mPtTyp; (2) lateral fibres of the middle portion (orange) and dorsal portion (red) of the mPtTyp; (3) medial fibres of the middle portion of the mPtTyp (green yellow). The transparency of all bone in the lateral view and the skull in the posterior view is at 80%. No fascia is present in this figure.
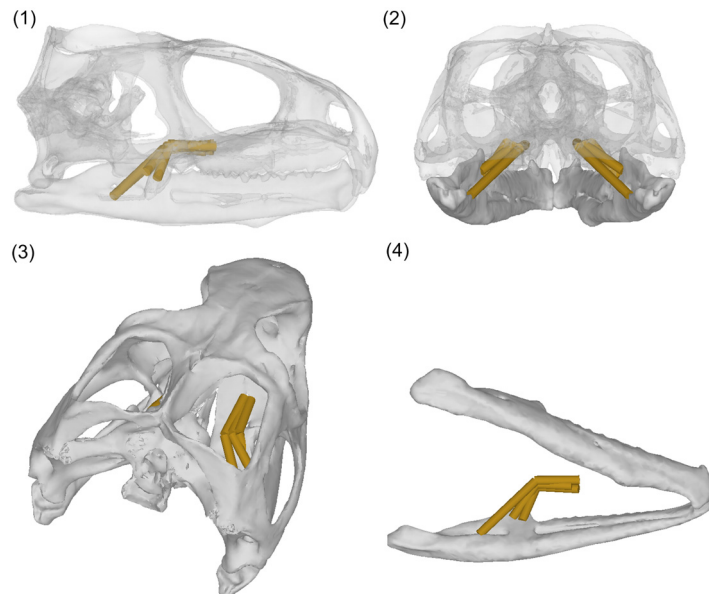

FIGURE 8. mPtATyp. (1) Lateral view with all bone at 80% transparency; (2) posterior view with the skull at 80% transparency; (3) posterodorsolateral view; (4) ventrolateral view of the lower jaw only. No fascia is present in this figure.
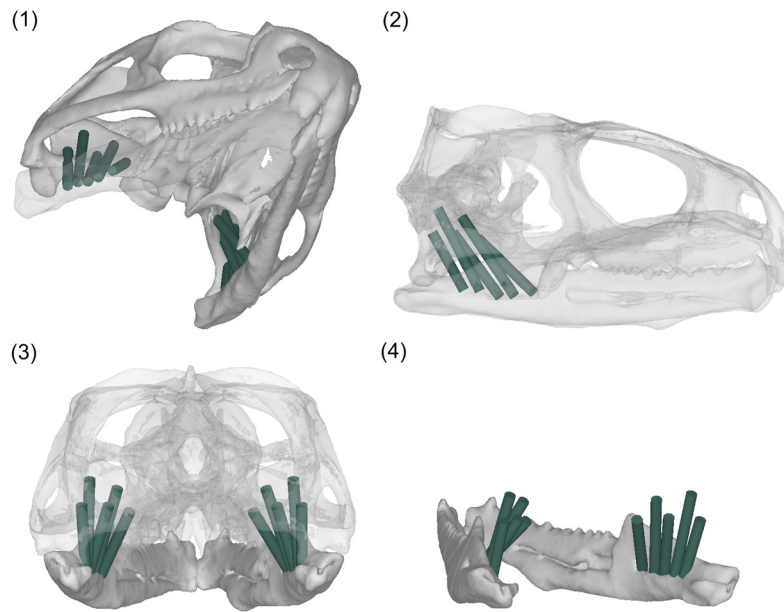
FIGURE 9. mAMP. (1) Anteroventrolateral view with the left side of the lower jaw at 80% transparency; (2) lateral view with all bone at 80% transparency; (3) posterior view with the skull at 80% transparency; (4) posterolateral view showing only the lower jaw. The fascia is not visible in this figure.
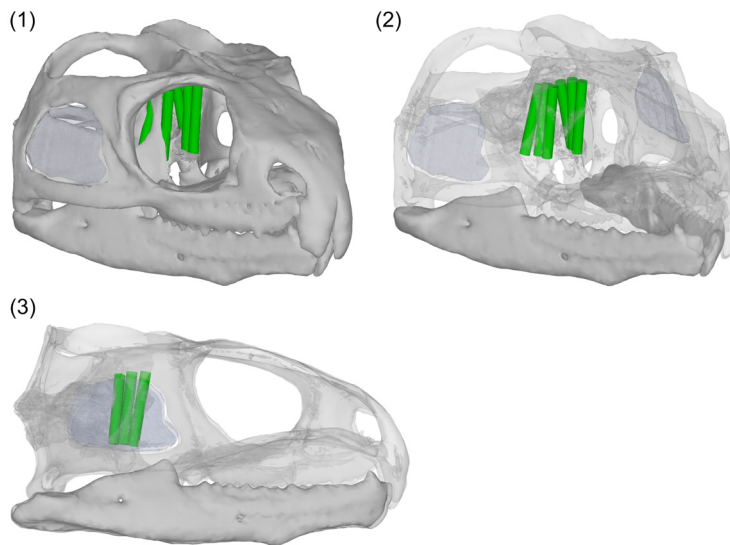

FIGURE 10. mLPt (1) Anterodorsolateral view; (2) anterodorsolateral view with the skull at 80% transparency; (3) lateral view with the skull at 80% transparency. Fascia at 80% transparency
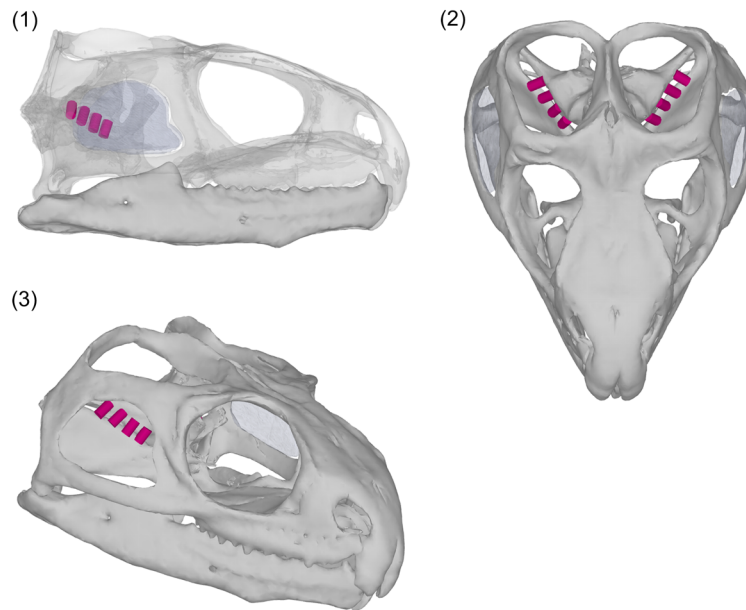
(1)

(2)

(3)

FIGURE 11. mPPt (1) Lateral view with the skull at 80% transparency; (2) dorsal view with a slight anterior tilt; (3) anterodorsolateral view. Where present the fascia is at 80% transparency.
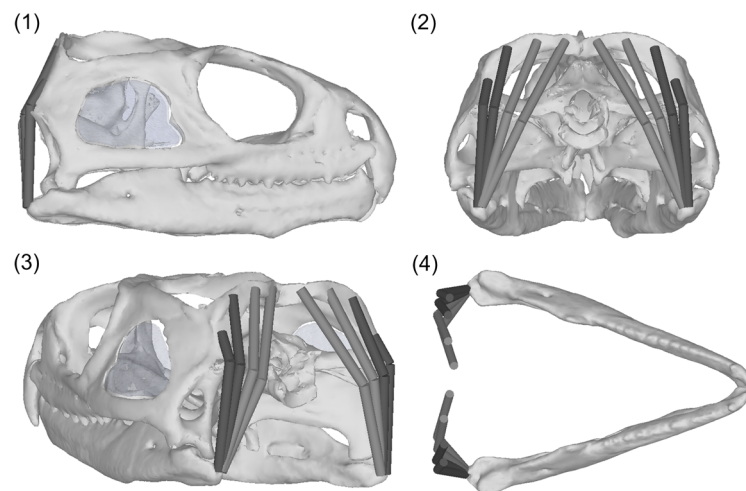
(1)

(2)

(3)

(4)

FIGURE 12. mDML (dark grey) and mDMM (light grey). (1) Lateral view; (2) posterior view; (3) posterolateral view; (4) dorsal view of only the lower jaw with a slight anterior tilt. Where present the fascia is at 80% transparency.

TABLE 2. Summary of all neck muscles modelled in this paper.

Muscle Group	Figure	Muscle Colour	Sections	Branching	Muscle Function
m. Trapezius (mTrap)	14	Purple	2	No	Holds or raises the head and some rotational control.
m. Episternocleidomastoid (mEscm)	14	Red	2	No	Holds or raises the head and some rotational control.
m. Clavicle Dorsalis (mClDo)	14	Peach	1	No	Holds or raises the head and some rotational control.
m. Spinalis Capitis (nSpCa)	15	Green	3	No	Holds or raises the head.
m. Axis-Supraoccipital (mAxSu)	16	Pink	3	No	Holds or raises the head.
m. Rectus Capitis Posterior Superficialis (mReCaPS)	16	Bright Blue	2	No	Holds or raises the head and slight rotational control.
m. Rectus Capitis Posterior Profundus (mReCaPP)	16	Light Blue	3	No	Holds or raises the head and rotational control.
m. Obliquus Capitis Magnus (mReCaM)	16	Blue Gray	3	No	Rotational control with limited contribution to raising the head.
m. Semispinalis Capitis (mSSpCa)	17	Brown	4	Yes	Holds or raises the head and rotational control.
m. Longissimus Capitis Lateralis (mLCaL)	17	Violet Red	1	Yes	Rotational control.
m. Longissimus Capitis Medialis (mLCaM)	17	Dark Red	2	No	Rotational control with limited contribution to raising the head.
m. Longissimus Capitis Pars Transversalis Cervicus (mLCaPTCe)	18	Navy Blue	1	Yes	Lowering the head and some rotational control.
m. Iliocostalis capitis (mIcosCa)	19	Bright Green	2	Yes	Lowering the head and some rotational control.
m. Longus Colli (mLoCol)	20	Yellow	7	No	Lowering the head and some rotational control.
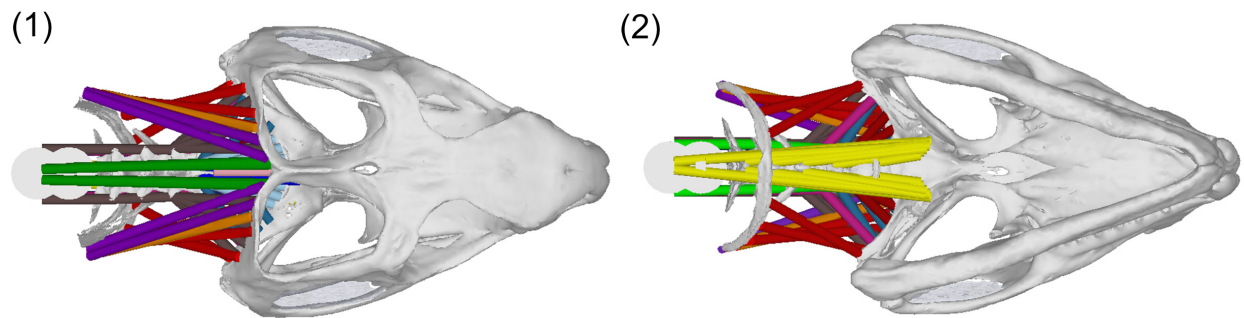
FIGURE 13. (1) Doral view and (2) ventral view of all major neck muscles.
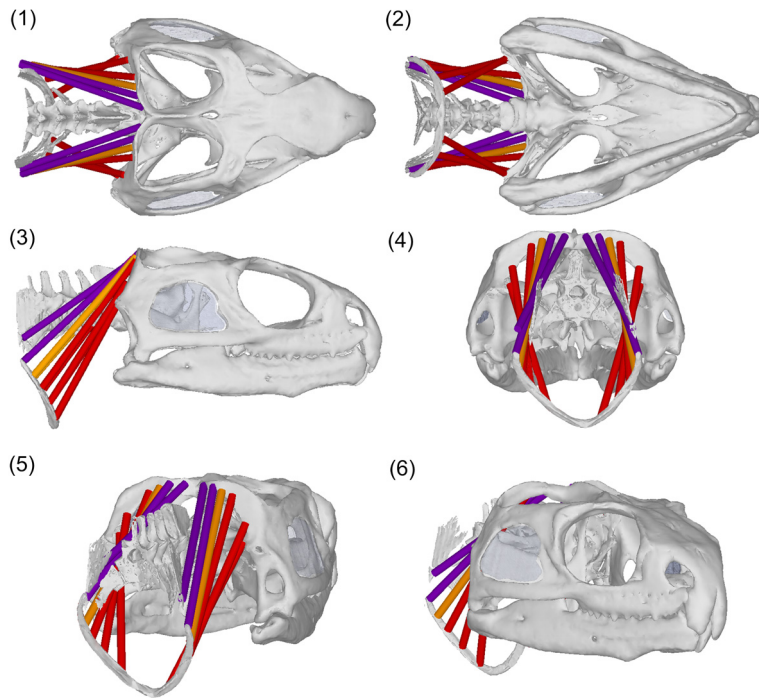
FIGURE 14. mTrap (purple), mEscm (red) and mClDo (peach). (1) Dorsal view; (2) ventral view; (3) lateral view; (4) posterior view; (5) posterolateral view; (6) anterolateral view. Fascia at 80% transparency.
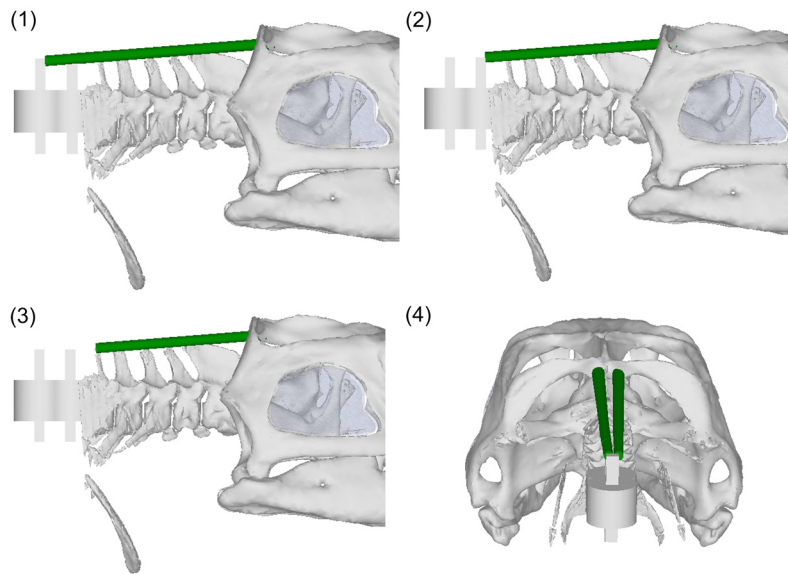

FIGURE 15. mSpCa. (1), (2) and (3) show posterior to anterior attachment locations on lateral views of the neck and posterior section of the skull; (4) posterodorsal view. Fascia at 80% transparency.
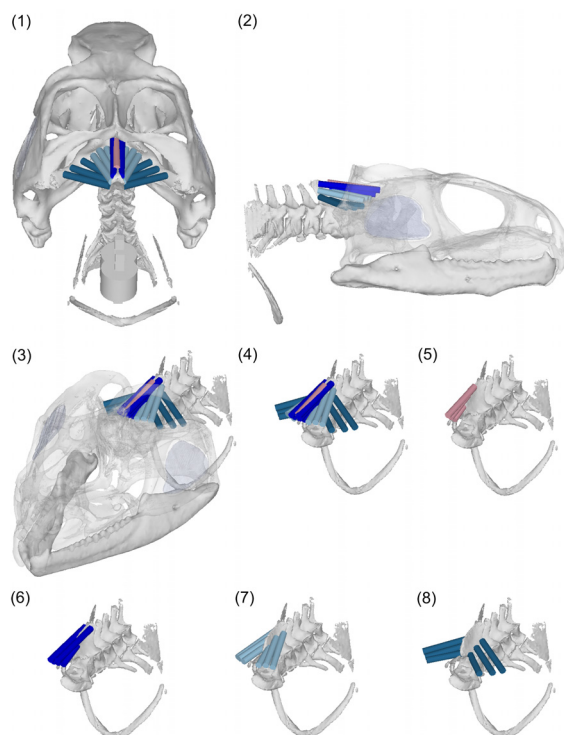
FIGURE 16. mAxSu (pink - [5]), mReCaPS (bright blue - [6]), mReCaPP (light blue [7]), mObCaM (blue gray [8]). (1) Posterodorsal view; (2) lateral view with the skull at 80% transparency; (3) anterodorsolateral view with the skull at 80% transparency; (4) anterodorsolateral view of only the neck showing all muscle groups; (5) anterodorsolateral view of only the neck showing the mAxSu; (6) anterodorsolateral view of only the neck showing the mReCaPS; (7) anterodorsolateral view of only the neck showing the mReCaPP; (8) anterodorsolateral view of only the neck showing the mObCaM. Where present the fascia is at 80% transparency.
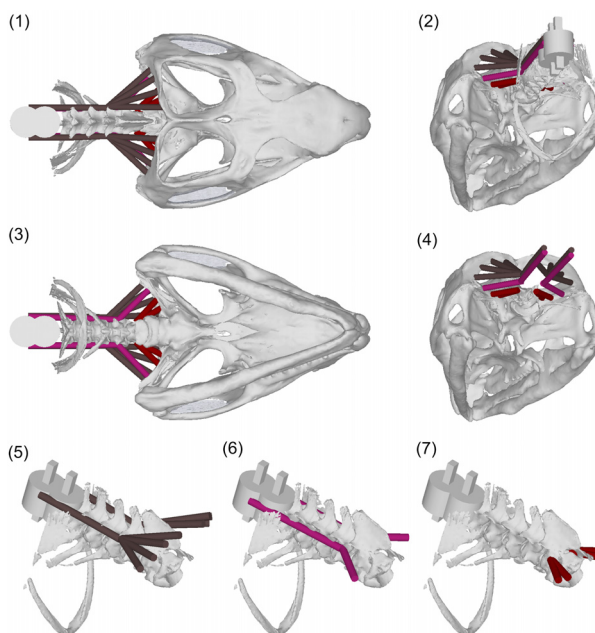

FIGURE 17. mSSpCa (brown [5]), mLCaL (violet_red [6]) and mLCaM (dark red [7]). (1) Dorsal view; (2) posteroventrolateral view; (3)ventral view; (4) posteroventrolateral view without the neck; (5) anterodorsolateral view of the mSSpCa without the skull; (6) anterodorsolateral view of the mLCaL without the skull; (7) anterodorsolateral view of the mLCaM without the skull. Where present the fascia is at 80% transparency.
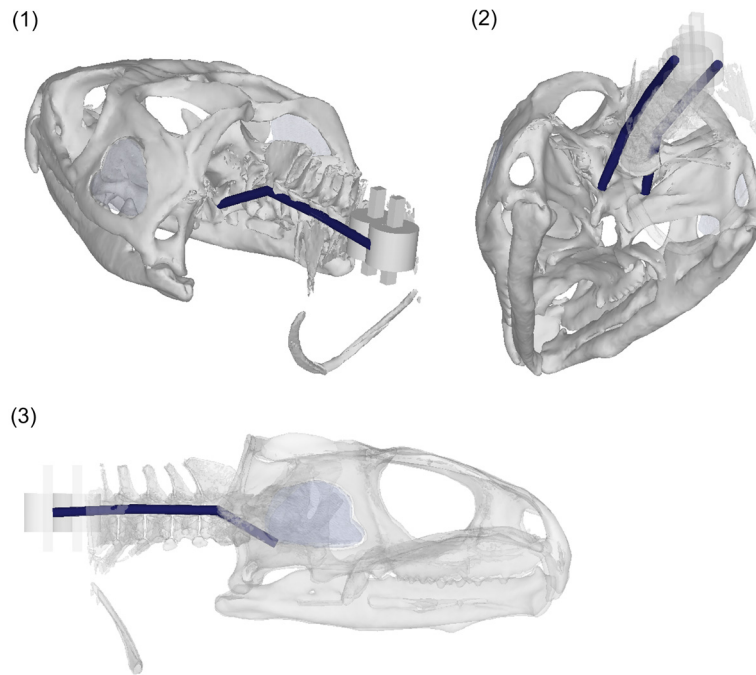
FIGURE 18. mLCaPTCe. (1) Posterodorsolateral view; (2) posteroventrolateral view with the neck at 80% transparency; (3) lateral view with all bone at 80% transparency. Fascia is at 80% transparency.

FIGURE 19. mlcosCa. (1) Posterodorsolateral view; (2) posteroventrolateral view with the neck at 80% transparency; (3) lateral view with all bone at 80% transparency. Fascia is at 80% transparency.
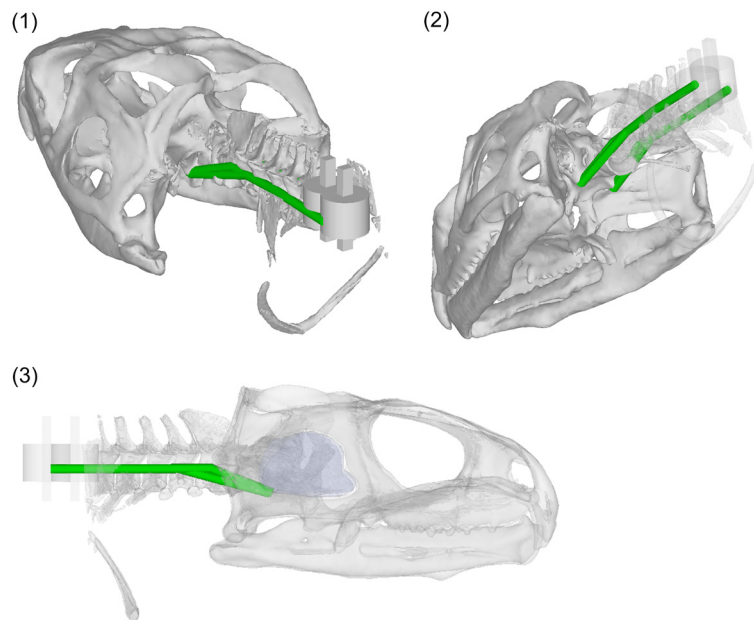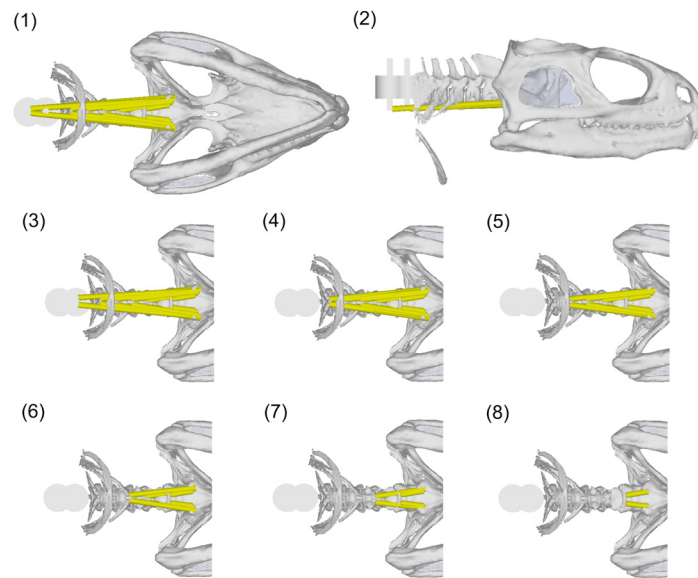
FIGURE 20. mLoCol. (1) ventral view of all muscle sections; (2) lateral view of all muscle sections; (3-7) ventral view of the neck and posterior part of the skull showing the attachment locations down the spine. Fascia is at 80% transparency.
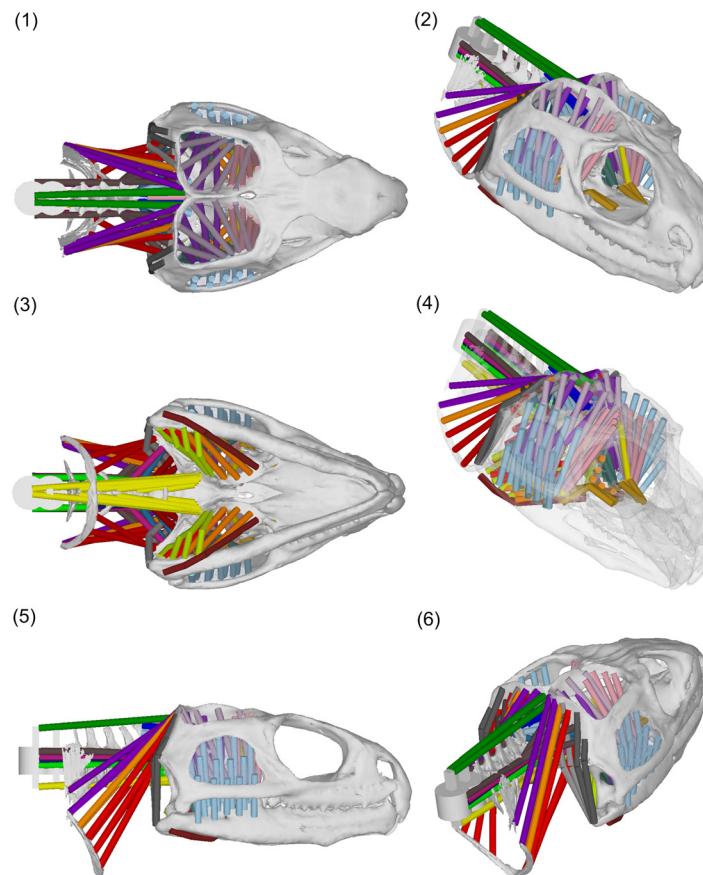

FIGURE 21. Full representation of the head and neck musculature in *Sphenodon*. (1) Dorsal view; (2) anterodorsolateral view; (3) ventral view; (4) anterodorsolateral view with all bone at 80% transparency; (5) lateral view; (6) posterodorsolateral view. Fascia at 80% transparency.
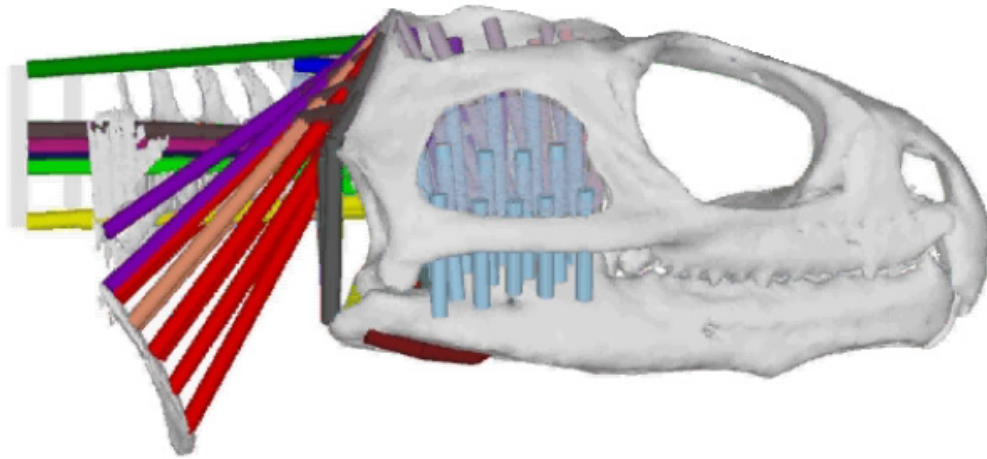
FIGURE 22. Rotating movie of the head and neck of *Sphenodon* showing all associated musculature. This animation is available on the website.
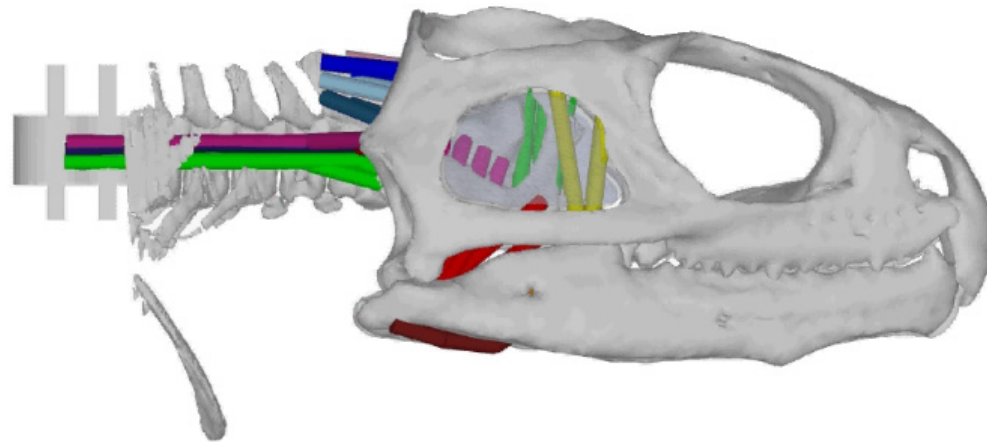

FIGURE 23. Rotating movie of the head and neck of *Sphenodon* where superficial muscle groups have been removed to reveal underlying structures. This animation is available on the website.

REFERENCES

Abdala, V. and Moro, S. 2003. A cladistic analysis of ten lizard families (Reptilia: Squamata) based on cranial musculature. *Russian Journal of Herpetology*, 10:53-73.

Adams, L.A. 1919. A memoir on the phylogeny of the jaw muscles in recent and fossil vertebrates, *Annals of the New York Academy of Science*, 28:51-166.

Al-Hassawi, A.M. 2004. *The osteology and myology of the craniocervical region in squamate reptiles: a comparative study*. Unpublished Ph.D. Thesis, University of London, UK.

Al-Hassawi, A.M. 2007. *Comparative Anatomy of the Neck Region in Lizards*. Trafford Publishing, Victoria, Canada.

Anderson, H.T. 1936. The jaw musculature of the phytosaur, *Machaeroprosopus*. *Journal of Morphology*, 59(3):549-587.

Barghusen, H.R. 1973. The adductor jaw musculature of *Dimetrodon* (Reptilia, Pelycosauria), *Journal of Paleontology*, 47:823-834.

Bryant, H.N., and Russell, A.P. 1992. The role of phylogenetic analysis in the inference of unpreserved attributes of extinct taxa. *Philosophical Transactions of the Royal Society of London B* 337:405-418.

Byerly, T.C. 1925. The myology of *Sphenodon punctatum*. *University of Iowa Studies in Natural History*, 9(6):1-51.

Conroy G.C., and Vannier, M.W. 1984. Noninvasive three-dimensional computer imaging of matrix-filled fossil skulls by high-resolution computed tomography. *Science*, 226 (4673):456-458.

Conroy, G., Vannier, M., and Tobias, P. 1990. Endocranial features of *Australopithecus africanus* revealed by 2- and 3-D computed tomography. *Science*, 247:838-841.

Curtis, N., Kupczik, K., O'Higgins, P., Moazen, M., and Fagan, M.J. 2008. Predicting skull loading: applying dynamics analysis to a macaque skull. *The Anatomical Record*, 291:491-501.

Curtis, N., Jones, M.E.H., Evans, S.E., Shi, J., O'Higgins, P., and Fagan, M.J. 2009. Predicting muscle activation patterns from motion and anatomy: modelling the skull of *Sphenodon* (Diapsida: Rhynchocephalia). *Journal of the Royal Society Interface*, published online. doi:10.1098/rsif.2009.0139.

Evans, D.C., Ridgely, R., and Witmer, L.M. 2009. Endocranial anatomy of Lambeosaurine Hadrosaurids (Dinosauria: Ornithischia): A sensorineural perspective on cranial crest function. *The Anatomical Record*, 292:1315-1337.

Fox, R.C. 1964. The adductor muscles of the jaw in some primitive reptiles. *University of Kansas Publishing Museum of Natural History*, 12:657-680.

Gasc, J.-P. 1981. Axial musculature, p. 355-435. In Gans C. and Parsons, T.S. (eds.). *Biology of the Reptilia volume 11*. Academic Press, New York and London.

Gauthier, J.A., Estes, R., de Queiroz, K. 1988. A phylogenetic analysis of the Lepidosauromorpha, p. 15-98. In Estes, R. and Pregill, G., (ed). *Phylogenetic Relationships of the Lizard Families: Essays Commemorating Charles L. Camp*. Stanford University Press, Stanford.

Gomes, N. 1974. Anatomie comparée de la musculature trigeminale des lacertilians, *Memoirs du Museum National d'Histoire Naturelle*, Paris (Zoology), 90:1-107.

Gorniak, G.C., Rosenberg, H.I., and Gans, C. 1982. Mastication in the tuatara, *Sphenodon punctatus* (Reptilia: Rhynchocephalia): Structure and activity of the motor system. *Journal of Morphology*, 171:321-353.

Grosse, I.R., Dumont, E.R., Coletta, C., Tolleson, A. 2007. Techniques for modelling muscle-induced forces on finite element models of skeletal structures. *The Anatomical Record Part A*, 290:1069-1088.

Günther, A. 1867. Contribution to the anatomy of *Hatteria* (Rhynchocephalus, Owen), *Philosophical Transactions of the Royal Society,* 157:1-34.

Haas, G. 1973. Muscles of the jaws and associated structures in the Rhynchocephalia and Squamata, p. 285-490. In Gans, C. and Parsons, T.S. (eds.), *Biology of the Reptilia volume 4*. Academic Press, New York and London.

Holliday, C.M. and Witmer, L.M. 2007. Archosaur adductor chamber evolution: integration of musculoskeletal and topological criteria in jaw muscle homology. *Journal of Morphology*, 268:457-484.

Holliday, C.M. 2009. New insights into dinosaur jaw muscle anatomy. *The Anatomical Record*, 292:1246-1265.

Hutchinson, J.R., Anderson, F.C., Blemker, S.S., and Delp, S.L. 2005. Analysis of hindlimb muscle moment arms in *Tyrannosaurus rex* using a three-dimensional musculoskeletal computer model: implications for stance, gait, and speed. *Paleobiology*, 31:676-701.

Jones, M.E.H., Curtis, N., Evans, S.E., O'Higgins, P., and Fagan, M.J. 2009. The head and neck muscles associated with feeding in *Sphenodon* (Reptilia: Lepidosauria: Rhynchocephalia). *Palaeontologia Electronica* 12 (2, 7A):1-56.

Moazen, M., Curtis, N., Evans, S.E., O'Higgins, P., and Fagan, M.J. 2008. Rigid-body analysis of a lizard skull: Modelling the skull of *Uromastyx hardwickii*. *Journal of Biomechanics*, 41:1274-1280.

Moazen, M., Curtis, N., Evans, S.E., O'Higgins, P., and Fagan, M.J. 2009. Assessment of the role of sutures in a lizard skull: a computer modelling study. *Proceedings of the Royal Society B*, 276:39-46.

Motani, R. 2005. Detailed tooth morphology in a durophagous ichthyosaur captured by 3D laser scanner. *Journal of Vertebrate Paleontology*, 25:462-465.

Nishi, S. 1916. Zur vergleichenden Anatomie der eigentlichen (genuinen) Rückenmuskeln. *Gegenbauers Morphologisches Jahrbuch*, 50:168-318.

Oelrich, T.M. 1956. The anatomy of the head of *Ctenosaura pectinata* (Iguanidae). Miscellaneous *Publications of Zoology University of Michigan,* 94:1-122.

Olson, E.C. 1961. Jaw mechanisms in rhipidistians, amphibians, reptiles. *American Zoologist*, 1:205-215.

Poglayen-Neuwall, I. 1953. Untersuchungen über die Trigeminusmuskulatur von *Hatteria*. *Zeitschrift wissenschaft Zoologie*, 157:57-76.

Rieppel, O. 2002. Feeding mechanics in Triassic stem-group sauropterygians: the anatomy of a successful invasion of Mesozoic seas. *Zoological Journal of the Linnean Society*, 135:33-63.

Schumacher, G.-H. 1973. The head muscles and hyolaryngal skeleton of turtles and crocodilians, chapter 2, p. 101-199. In Gans, C. and Parsons, T.H. (eds.), *Biology of the Reptilia 4 Morphology*. Academic Press, London and New York.

Schwenk, K. 1986. Morphology of the tongue in the tuatara, *Sphenodon punctatus* (Reptilia: Lepidosauria), with comments on function and phylogeny. *Journal of Morphology* 188:129-156

Snively, E. and Russell, A.P. 2007. Functional variation of neck muscles and their relation to feeding style in Tyrannosauridae and other large theropod dinosaurs. *The Anatomical Record*, 290:934-957.

Strait, S.G. and Evans, A.R. 2008. Special Issue: Three-Dimensional imaging in vertebrate paleontology. *Palaeontologia Electronica*, 11(2).

Sutton, M.D. 2008. Tomographic techniques for the study of exceptionally preserved fossils. *Proceedings of the Royal Society B: Biological Sciences*, 275:1-7.

Throckmorton, G.S. 1978. Action of the pterygoideus muscle during feeding in the lizard *Uromastix aegyptius* (Agamidae). *The Anatomical Record*. 190:217-222.

Tsuihiji, T. 2005. Homologies of the transversospinalis muscles in the anterior presacral region of Sauria (crown Diapsida). *Journal of Morphology*, 263:151-178.

Tsuihiji, T. 2007. Homologies of the longissimus, iliocostalis, and hypaxial muscles in the anterior presacral region of extant Diapsida. *Journal of Morphology*, 268:986-1020.

Wickens, Z. 2007. Computer aided visualisation in palaeontology (Meeting report). *Palaeontological newsletter*, 66:37-40.

Witmer, L.M. 1995. The extant phylogenetic bracket and the importance of reconstructing soft tissues in fossils, p. 19-–33. In Thomason, J.J. (ed), *Functional Morphology in Vertebrate Palaeontology*. Cambridge University Press, Cambridge.

Witmer, L.M. and Ridgely, R.C. 2008. The paranasal air sinuses of predatory and armoured dinosaurs (Archosauria: Theropoda and Ankylosauria) and their contribution to cephalic structure. *The Anatomical Record*, 291:1362-1388.

Witmer, L.M. and Ridgely, R.C. 2009. New insights into the brain, braincase, and ear region of tyrannosaurs (Dinosauria, Theropoda), with implications for sensory organization and behavior. *The Anatomical Record*, 292:1266-1296.

Wu, X.-C. 2003. Functional morphology of the temporal region in the Rhynchocephalia. *Canadian Journal of Earth Sciences*, 40:589-607.